Extended Abstracts of the 2014 International Conference on Solid State Devices and Materials, Tsukuba, 2014, pp854-855

n^+/p^+-Single Doping Effects on Impurity Band Structure Modulation in Two Dimensional Si Layers

T. Mizuno, Y. Nakahara, Y. Nagamine, Y. Suzuki, Y. Nagata, T. Aoki, and T. Sameshima*
Kanagawa Univ., Hiratsuka, Japan (mizuno@info.kanagawa-u.ac.jp), * Tokyo Univ. of Agric. and Tech., Koganei, Japan

Abstract

We experimentally studied n^+/p^+ single dopant atom effects on band structure modulation in 2D-Si layers in a wide range of dopant density N, using photoluminescence (PL) method. Bandgap E_G of both n^+/p^+ 2D-Si strongly depends on the N, and decreases with increasing N, which is attributable to E_G narrowing effects δE_G. However, δE_G in the doped 2D-Si is much smaller than that of 3D-Si and depends on the dopant type. We introduce a simple model for the small δE_G, considering the impurity band structure modulation in a heavily doped 2D-Si. Moreover, small PL polarization of doped 2D-Si is also discussed.

I. Introduction

In two dimensional (2D) Si layers, which are key structures for realizing extremely-thin SOIs (ETSOIs) and FinFET CMOS [1], as well as Si photonic devices [2], we experimentally demonstrated phonon confinement effects (PCE) caused by the Heisenberg's uncertainty principle of the phonon wave vector and bandgap (E_G) expanding due to electron confinement effects [3]- [5]. Moreover, in the case of an n^+ 2D-Si in less than 4×10^{20}cm^{-3}, PL method show that δE_G is reduced [5], compared to that of 3D-Si [6]. The δE_G of 3D-Si is attributable to the impurity band of donors including the band tailing [7]. Moreover, donor level modulation in an 1D-Si is reported [8]. To design a pn junction of CMOS composed of 2D-Si in detail, it is strongly required to clarify both the reduced δE_G effects in detail and the physical mechanism in both n^+ and p^+ 2D-Si in a wide range of dopant density.

In this work, we experimentally studied the n^+/p^+ single dopant atom effects on the band structures in doped 2D-Si layers fabricated by ion implantation, using PL method. We confirmed that E_G strongly depends on an impurity dopant density N, decreases with increasing the N in both n^+/p^+ 2D-Si layers, but δE_G in doped 2D-Si is much smaller than that in doped 3D-Si. The reduced δE_G in doped 2D-Si is possibly attributable to the impurity band E_I modulation (IBM) effects in doped 2D-Si. Next, we show small PL polarization in a doped 2D-Si, which is possibly caused by the disturbed crystal direction due to heavy impurity dopant.

II. Experimental for Doped 2D-Si Layers

To control 2D-Si thickness T_S very well, n^+ and p^+ 2D-Si layers were fabricated by two-step (low-temperature (T) after high-T oxidation) thermal oxidation induced thinning of (100) bonded SOI substrates **(Figs.1 and 2)**. In addition, P^+ for donor and B^+ for acceptor ions were implanted in different process steps **(Figs.1 and 2)**, considering that the P^+ and B^+ segregation coefficients m at the Si/SiO_2 interface, during the oxidation of SOI substrates, are about 10 and 0.1, respectively [5], [9].

HRTEM observation shows very uniformity and good crystal quality of n^+ 2D-Si layer even at higher N condition **(Fig.3)**, which is the same image as HRTEM result of intrinsic 2D-Si [3].

SIMS results for boron profile in a doped 2D-Si show that average of experimental boron density $\overline{N_B}$ is almost the same as the 2D simulation results [10] **(Fig.4)**, although the SIMS profile at the oxide/Si interfaces is inaccurate, because of the SIMS detection limit. Thus, in this study, N of 2D-Si in various ion implantation conditions can be obtained by the simulation results [10].

We analyzed the E_G properties of n^+/p^+ 2D-Si evaluated by PL method with 2.33eV excitation laser at room temperature [4]. Laser power P_L was 1mW to compress the P_L heating of Si [4], and the laser diameter is 1μm.

III. Dopant Density Dependence of δE_G

N dependence of PL spectra shows that PL intensity I_{PL} and E_G in both n^+/p^+ 2D-Si decreases with increasing N **(Figs.5 and 6)**, where $E_G \propto N^{-0.009}$ in both n^+/p^+ 2D-Si **(Fig.6)**. However, the N dependence in p^+ 2D-Si is much different from that of n^+ 2D-Si **(Fig.6)**. The reduced E_G in both n^+/p^+ 2D-Si is attributable to the δE_G caused by the impurity band in a degenerate Si [7], [8]. Here, $\delta E_G \equiv E_{GI} - E_{GD}$, where E_{GI} and E_{GD} are E_G of intrinsic and doped 2D-Si, respectively **(Figs.6-8(a))**. δE_G of n^+ 2D-Si is much smaller than that of 3D-Si ($\delta E_G = 18.7\ln(N/7\times10^{17})$ [6], and the δE_G of n^+ 2D-Si can be well fitted by the following equation **(Fig.7)**:

$$\delta E_G = 15.7\ln(N/3.32\times10^{19}). \quad (1)$$

Thus, the coefficient of N in Eq.(1) is larger by about two orders of magnitude than that of 3D-Si [6]. However, δE_G difference between p^+ 2D-Si and 3D-Si is very small **(Fig.7)**. Consequently, the reduced δE_G is the characteristic of doped 2D-Si, and depends on the dopant type.

IV. Impurity Band Modulation (IBM) of Doped 2D-Si

To explain the δE_G difference between 2D- and 3D-Si **(Fig.7)**, we consider that there are two possible mechanisms. One is the donor deactivation effects in the 2D-Si, and the other is IBM. Using the former model, the donor activation rate in the 2D-Si should be reduced by about two orders of magnitude, compared to that of 3D-Si **(Fig.7)**. However, the possibility of the above larger deactivation is very low, because even in 1D-Si, the donor activation rate is reduced by only one order of magnitude [8]. Thus, we introduce the IBM model in this study **(Fig.8)**.

Doped 2D-Si has a step function of density of states (DOS) due to the quantum confinement effects of electrons, whereas $DOS(E) \propto \sqrt{E}$ in the 3D-Si [6]. E_I including the band tailing causes the δE_G [7] **(Fig.8)**. The bandwidth of E_I, ΔE_I expands with increasing donor concentration N_D [10], resulting in the δE_G increase **(Fig.7)**. On the other hand **(Fig.8 (b))**, ΔE_I of n^+ 2D-Si becomes possibly narrower by δE_I, resulting in the δE_G reduction in the doped 2D-Si. Namely, since $E_G = E_C - E_V - \delta E_G$ in a doped Si **(Fig.8 (a))**, δE_G of doped 2D-Si, $\delta E_{G\text{-}2D}$ can be expressed by $\delta E_{G\text{-}3D}$ of 3D-Si. That is **(Fig.8 (a))**,

$$\delta E_{G-2D} = \delta E_{G-3D} - \delta E_I \quad (2),$$

where δE_I is the IBM in 2D-Si.

Using Eq.(2) and Fig.7 data, δE_I can be estimated in both n^+/p^+ 2D-Si layers **(Fig.9)**. δE_I is independent of N, but δE_I of n^+ 2D-Si (~81meV) is much larger than that of p^+ 2D-Si (~26meV). This suggests that δE_I strongly depends on the impurity type of donor or acceptor. Physical mechanism for δE_I is not understood at present, but is possibly due to band tailing [7] reduction in the 2D-Si, since the donor's ionization energy increases in the case of 1D-Si [8], and thus this tendency is opposite to the experimental data.

V. PL Polarization of Doped 2D-Si

In an intrinsic 2D-Si, PL intensity is polarized [12], which is considered to be attributable to some optical anisotropic-properties of 2D-Si quantum well which relates to the crystal direction [13]. Even in a doped 2D-Si, PL intensity is also polarized **(Fig.10)**. In addition, the PL polarization degree P, defined by $P(\theta) \equiv \left(I_{PL}(0^\circ) - I_{PL}(\theta)\right)/\left(I_{PL}(0^\circ) + I_{PL}(\theta)\right)$ (0° shows the [110] direction) is almost independent of dopant density and impurity type, but is smaller than that of intrinsic 2D-Si **(Fig.11)**. Thus, heavily dopant atoms affect the optical anisotropic-properties and crystal quality of 2D-Si.

On the other hand, PL peak energy of the doped 2D-Si is independent of the crystal direction **(Fig.12)**, similar to 2D i-Si [12].

VII. Conclusion

We experimentally studied n^+/p^+ dopant atom effects on E_G in 2D-Si layers in a wide range of N, using PL method. E_G of both n^+/p^+ 2D-Si decreases with increasing N, which is attributable to E_G narrowing effects δE_G. However, δE_G in the doped 2D-Si is much smaller than that of 3D-Si, and depends on the dopant type. We introduce a simple model for the small δE_G, considering the impurity band structure modulation (IBM) in a heavily doped 2D-Si. Consequently, using the detailed E_G properties of the doped 2D-Si, we can precisely design a pn junction structure for future CMOS composed of 2D-Si.

Acknowledgement: We would like to thank Prof. J. Nakata and Dr. Y. Hoshino of Kanagawa Univ. for ion implantation. This work was partially supported by KAKENHI (24560422).

References:[1] J.-P.Colinge, *SILICON-ON-INSULATOR TECHNOLOGYOI*, (Kluwer Academic Publishers) 2004. [2] S. Saito, IEDM 2008, Paper 19.5. [3] T. Mizuno, JJAP **51**, 02BC03, 2012. [4] T. Mizuno, JJAP **52**, 04CC13, 2013. [5] T. Mizuno, JJAP **53**, 04EC08, 2014. [6] S. M. Sze, *Physics of Semiconductor Devices* (Wiley), 2007. [7] D.S. Lee, IEEE TED **30**, 626, 1983. [8] M.T. Björk, Nature Nanotech. **4**, 103, 2009. [9] A.S. Grove, *Physics and Technology of Semiconductor Devices* (Wiley) 1967. [10] www.silvaco.com. [11] H.Ikeda, APL **96**, 012106, 2010. [12] T. Mizuno, JJAP **53**, 04EC09, 2014. [13] Y. Kanemitsu, Phys. Rev. B **56**, R15 561 (1997).

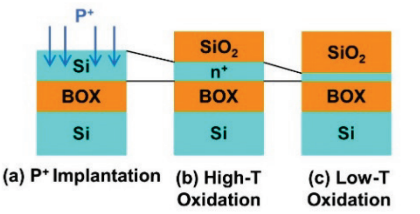

Fig.1 Schematic two-step oxidation fabrication process for 2D-n$^+$ layers. (a) After P$^+$ implantation into (100)SOI, (b) Si was thinned by high temperature oxidation (1000°C). (c) Additional low-T oxidation (900°C) after (b) was carried out to form nm-region thick Si layer.

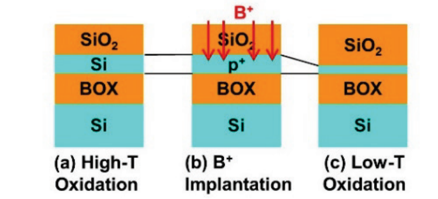

Fig.2 Schematic two-step oxidation fabrication for 2D-p$^+$ layers. (a) After high-T oxidation process (1000°C), (b) B$^+$ was implanted into thinned (100)SOI. (c) Additional low-T oxidation (900°C) after (b) was carried out to form nm-region thick Si layer.

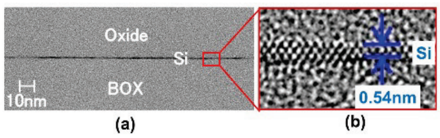

Fig.3 HRTEM observation of cross section of 2D-n$^+$ layer with N_D=4×10^{20}cm^{-3}. (a) Very uniform 2D-n$^+$ layer, and (b) good Si lattice image and T_S≈0.54nm.

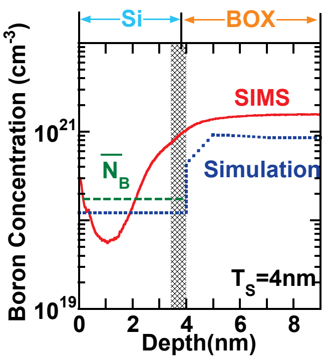

Fig.4 SIMS (solid line) and simulation distribution (dotted line) for boron atoms, where boron dose is 1×10^{16}cm^{-2} and T_S=4nm. Minimum T_S for SIMS detection limit is about several nm. Dashed line shows the experimental average of boron density (1.8×10^{20}cm^{-3}) in Si layer which is obtained by the SIMS data, and is almost the same level as the simulation result (1.2×10^{20}cm^{-3}) in Si.

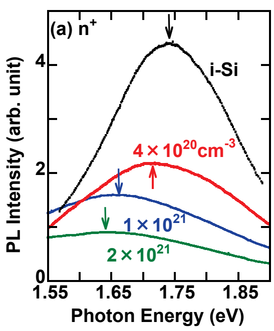

Fig. 5(a)

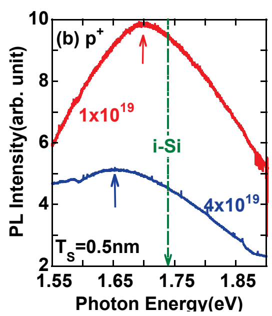

Fig.5 Dopant density dependence of PL spectra of (a) n$^+$ and (b) p$^+$ 2D-Si, where T_S=0.5nm. Dotted and dashed line in (b) shows the E_{PH} of i-Si.

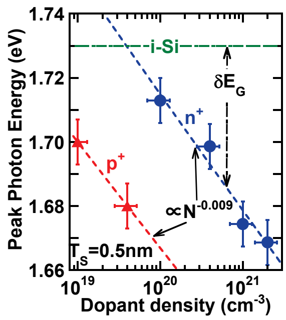

Fig.6 E_{PH} vs. simulated impurity density of n$^+$ (circles) and p$^+$ 2D-Si (triangles), where T_S=0.5nm. Dotted and dashed line shows the E_{PH} of i-Si. Vertical and lateral error bars show the PL resolution and N accuracy (Fig.4 data) in this study. Dashed line shows the fitting curve of $E_G \propto N^{-0.009}$, where the correlation coefficient is 0.98.

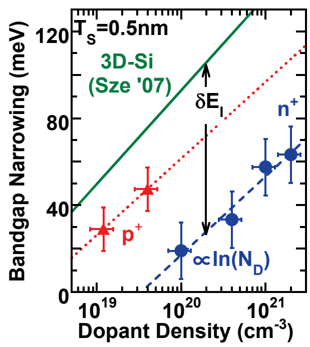

Fig.7 Bandgap narrowing vs. simulated impurity density of n$^+$ (circles) and p$^+$ 2D-Si (triangles), where T_S=0.5nm. Solid line shows empirically formula of 3D-Si [6]. Dashed line shows the fitting curve of $\delta E_G = 15.7\ln(N_D/3.32\times10^{19})$ in n$^+$ 2D-Si with the correlation coefficient of 0.98. δE_I is E_I modulation in n$^+$ 2D-Si.

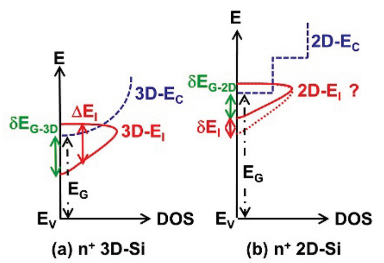

Fig.8 Schematic density of states functions (E vs. DOS) for (a) n$^+$ 3D-Si [7] and (b) n$^+$ 2D-Si with expanded E_G. Dashed and solid lines show the conduction and impurity bands, respectively. Dotted line in (b) shows the impurity band of 3D-Si. δE_G, ΔE_I and δE_I are E_G narrowing, E_I band width and E_I modulation, respectively.

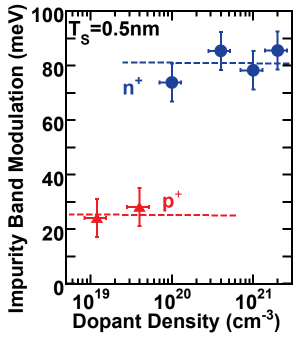

Fig.9 Impurity band structure modulation of n$^+$ (circles); δE_{IN} and p$^+$ 2D-Si (triangles); δE_{IP} as a function of simulated dopant density, where T_S=0.5nm. Both δE_{IN} and δE_{IP} are independent of dopant density, but δE_{IN} is much larger than δE_{IP}.

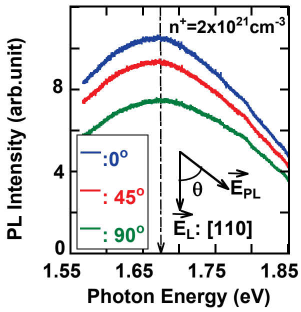

Fig.10 Polarization PL spectra of 2D-n$^+$ layer in various θ, where N=2×10^{21}cm^{-3} and T_S=0.5nm. $\overrightarrow{E_L}$ at fixed [110] direction and $\overrightarrow{E_{PL}}$ in the inset show polarization laser and PL vectors, respectively, and θ is the angle between $\overrightarrow{E_L}$ and $\overrightarrow{E_{PL}}$.

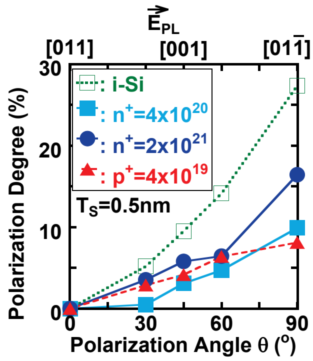

Fig.11 PL polarization degree of n$^+$ (solid lines), p$^+$ (dashed line), and intrinsic 2D-Si (dotted line) at $\overrightarrow{E_L}$ = [110] as a function of θ, where T_S=0.5nm.

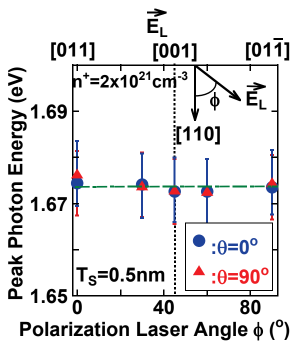

Fig.12 ϕ dependence of E_{PH} at θ=0° (circles) and 90° (triangles), where N=2×10^{21}cm^{-3} and T_S=0.5nm. Inset shows the polarization laser angle ϕ between [110] direction and $\overrightarrow{E_L}$.